Title

Inter- and intra-rater reliability of patellofemoral kinematic and contact area quantification by fast spin echo MRI and correlation with cartilage health by quantitative T1ρ MRI

Journal

The Knee, 23(1)

ISSN

0968-0160

Authors

Lau, Brian C
Thuillier, Daniel U
Pedoia, Valentina
et al.

Publication Date

2016

DOI

10.1016/j.knee.2015.08.017

Peer reviewed

HHS Public Access

Author manuscript

Knee. Author manuscript; available in PMC 2016 February 22.

Published in final edited form as:

Knee. 2016 January ; 23(1): 13–19. doi:10.1016/j.knee.2015.08.017.

Inter- and intra-rater reliability of patellofemoral kinematic and contact area quantification by fast spin echo MRI and correlation with cartilage health by quantitative T1ρ MRI☆

Brian C. Lau[*,a], **Daniel U. Thuillier**[a], **Valentina Pedoia**[b], **Ellison Y. Chen**[b], **Zhihong Zhang**[b], **Brian T. Feeley**[a], and **Richard B. Souza**[c]

[a]UCSF Department of Orthopaedic Surgery, United States

[b]UCSF Department of Radiology and Biomedical Imaging, United States

[c]UCSF Department of Physical Therapy and Rehabilitation Science, United States

Abstract

Background—Patellar maltracking is a leading cause of patellofemoral pain syndrome (PFPS). The aim of this study was to determine the inter- and intra-rater reliability of a semi-automated program for magnetic resonance imaging (MRI) based patellofemoral kinematics.

Methods—Sixteen subjects (10 with PFPS [mean age 32.3; SD 5.2; eight females] and six controls without PFPS 19 [mean age 28.6; SD 2.8; three females]) participated in the study. One set of T2-weighted, fat-saturated fast spin-echo (FSE) MRIs were acquired from each subject in full extension and 30° of knee flexion. MRI including axial T1ρ relaxation time mapping sequences was also performed on each knee. Following image acquisitions, regions of interest for kinematic MRI, and patellar and trochlear cartilage were segmented and quantified with in-house designed spline- based MATLAB semi-automated software.

Results—Intraclass Correlations Coefficients (ICC) of calculated kinematic parameters were good to excellent, ICC > 0.8 in patellar flexion, rotation, tilt, and translation (anterior -posterior, medial -lateral, and superior -inferior), and contact area translation. Only patellar tilt in the flexed position and motion from extended to flexed state was significantly different between PFPS and control patients ($p = 0.002$ and $p = 0.006$, respectively). No significant correlations were identified between patellofemoral kinematics and contact area with T1ρ relaxation times.

Conclusions—A semi-automated, spline-based kinematic MRI technique for patellofemoral kinematic and contact area quantification is highly reproducible with the potential to help better understand the role of patellofemoral maltracking in PFPS and other knee disorders.

Keywords

Patellofemoral kinematics; MRI; T1ρ; Reliability

☆Funding — NIH/NIAMS P50 AR060752 Orthopaedic Research and Education Foundation Resident Research Project.

*Corresponding author at: 500 Parnassus Avenue, #MU320W, San Francisco, CA 94143, United States. Tel.: +1 415 476 6043; fax: +1 415 476 1304. laub@orthosurg.ucsf.edu (B.C. Lau)..

7. Conflicts of interests The authors declare that they have no conflict of interest.

1. Introduction

Patellofemoral pain syndrome (PFPS) is common and affects approximately 25% of the population with long term anterior knee pain [15]. The prevailing thought is that PFPS is the result of abnormal kinematics of the patella which may alter the contact area and distribution of loads across the patellofemoral joint [19,22]. Abnormal patellofemoral contact caused by maltracking may trigger cartilage degeneration [5,22]. In fact radio-graphic patellofemoral joint osteoarthritis may be more common than tibiofemoral osteoarthritis in community-based studies [8,29]. Some studies also suggest that patellofemoral osteoarthritis may be more strongly associated with knee symptoms than tibiofemoral osteoarthritis [12,13].

There are surgical options available to alleviate pain associated with patellofemoral maltracking including arthroscopic lateral retinacular release or an anteromedialization of the tibial tuberosity, Fulkerson procedure [1,4,10,25]. PFPS, however, may be the result of many other etiologies (e.g. overuse, abnormal lower extremity kinematics) and clinicians must be able to differentiate PFPS caused by maltracking.

Normal patellar tracking is a dynamic process that is dependent on the degree of knee flexion. The patella undergoes changes in tilt, rotation, and medial-lateral position as the knee goes through a range of motion. A prior study found that patients with maltracking had greater patellar tilt and lateral displacement during knee flexion in patients with PFPS compared to healthy controls [23].

Traditional clinical strategies to determine patellar maltracking include patellar laxity and J-sign [15]. Sunrise plain films are also used to highlight patellar tilt and computed tomography (CT) scans can determine excessive patellar lateralization through the trochlear groove tibial tubercle (TG/TT) distance [15]. The TG/TT distance can also be determined on conventional magnetic resonance imaging (MRI). Conventional radiographs, CT scans, and MRIs are limited as they only assess patients in a single knee position and, as previously described, patella movement changes with changes from in knee extension to flexion.

Recently there has been an increased focus on utilizing kinematic MRI techniques to evaluate patellofemoral joint motion [3,9,18,20,23,30–32]. Prior studies have utilized kinematic MRI techniques to determine the in vivo patellar motion such as patellar tilt or translation (anterior-posterior, medial-lateral, and superior-inferior directions) or total patellofemoral joint contact area in PFPS and controls through a defined knee range of motion [3,9,18,20,23,30–32]. To our knowledge no technique quantifies in-vivo contact area translation. Established techniques are also limited in that there is not a unified technique that simultaneously measures patellar kinematics and contact area size with translation. Furthermore, the reproducibility of prior techniques for future studies is limited as several techniques did not report inter-user reliability.

Additionally, no studies have correlated in-vivo MRI patellar kinematics with patellofemoral cartilage degeneration. Quantitative T1ρ MRI evaluates proteoglycan content in articular cartilage with prolonged relaxation times indicating increased cartilage degeneration and has been shown as a reliable and sensitive modality to detect early degeneration [7,16,24,26–28]. One prior study has evaluated T1ρ relaxation times in patellofemoral pain patients [30]

and found greater cartilage degeneration in the lateral facet of the patellar cartilage in patients with PFPS compared to healthy controls [30]. The prior study also found a strong correlation between greater lateral patellar tilt and greater lateral facet cartilage degeneration [30]. To our knowledge, no prior studies have associated in-vivo MRI kinematics with quantitative T1ρ MR relaxation times in people with PFPS.

The primary purpose of this study was to evaluate the inter- and intra-user reliability of patellofemoral kinematic and contact area with an MRI based in-vivo technique. Our primary hypothesis is that the spline-based MRI based in-vivo technique will demonstrate excellent inter- and intra-user reliability. The secondary purpose is to compare patellofemoral kinematics between PFPS and control patients from extension to flexion. We hypothesize that PFPS will have greater lateral displacement from extension to flexion. The third aim of this study is to correlate patellofemoral kinematic and contact area with cartilage degeneration as determined by T1ρ imaging. Our hypothesis is that greater lateral patella tilt and lateral translation, and lateralization of the contact area in PFPS will correlate with greater cartilage degeneration in the lateral patella.

2. Material and methods

This study was approved by the Committee on Human Research at our institution. We performed a cohort, cross-sectional study with PFPS patients recruited from a sports medicine clinic at a single academic institution. Control subjects were solicited through flyers posted at our institution's sports medicine clinic. All subjects provided written informed consent for enrollment in the study.

2.1. Inclusion and exclusion criteria

The inclusion criteria for this study included skeletally mature patients aged 18 to 45 with anterior knee patellofemoral pain with no evidence of osteoarthritis (Kellgren-Lawrence grade 0). All patients were examined by a sports medicine fellowship trained orthopedic surgeon and had other causes of knee pain ruled out by history and physical exam. PFPS pain was confirmed clinically with reproduction of symptoms with resisted knee extension. Patellar maltracking was determined by patellar tilt on a 30° Merchant radiograph of the affected knee. The patellar tilt angle was defined as the angle between a line connecting the medial and lateral edges of the patella and the horizontal when measured on a Merchant radiograph at 30° of flexion. Patients were included if their patellar tilt was N5° and b25°. Patients were excluded if they did not meet the inclusion criteria or if they had previous surgeries or injuries to the involved knee including previous patellar dislocations, or had any contraindications for MRI. Patients with any evidence of prepatellar bursitis or large joint effusion were also excluded. Control patients were excluded if they had a history of knee injury, surgery, or any knee pain.

2.2. Kinematic MRI acquisition and processing protocol

MRI was performed using a 3 T scanner (General Electric, WI), an 8-channel phased array TR knee coil, and an in-house built loading apparatus mounted on the scanner table (Fig. 1). Subjects were positioned supine on top of the loading apparatus. Two sets of MR images

(sagittal T2-weighted fat-saturated fast spin-echo (FSE) images with TR/TE = 4300/51 ms, FOV = 14 cm, matrix = 512 × 256 slice thickness = 2.5 mm, gap = 0.5 mm, echo train length [ETL] = 9, bandwidth = 31.25 kHz, and NEX = 2) of one knee (controls: left knee; patients: knee with worse anterior knee patellofemoral pain) were acquired. The first set of images were acquired in full extension (0°) with 25% of the subject's weight load applied at the bottom of subjects' foot by a footplate through a pulley system, and the next set was acquired in 30° of knee flexion with the same amount of load.

Femoral and patellar bone regions of interest were segmented on FSE images using a software program developed in-house using a spline-based semi-automated (automated edge detection and manual correction) segmentation algorithm in MATLAB (Mathworks Inc, CA), Fig. 2. Regions of interests that were segmented in the fully extended position included the femoral bone, femoral condyles, patellar bone, patellofemoral contact area, femoral axis, and patellar axis. In the flexed position, the regions of interests that were segmented include the femoral bone, patellar bone, and patellofemoral contact area.

To establish the patellar coordinate system (PCS), the ML_P axis of the patella was defined by connecting the centers of the most medial and lateral slices of the patella. The midpoint of the line served as the origin for the PCS. The long axis of the patella extended from the inferior apex of the patella in a direction parallel to the back surface of the patella and was manually defined on the mid-sagittal slice of the patella. The anterior-posterior (AP_P) axis of the patella was defined by taking the cross product between the ML_P axis and the long axis of the patella. The superior-inferior (SI_p) axis of the patella was then defined by taking the cross product between the ML_P and AP_P axes, providing an anatomic axis for the patella (Fig. 3). Similarly, the femoral coordinate system (FCS) was established by fitting spheres to the contours defining the posterior surfaces of the femoral condyles using a least-squares fitting algorithm. The line joining the two sphere centers defined the medio-lateral axis (ML_F) axis, and the midpoint of this line served as the origin for the femoral coordinate system (Fig. 4). The femoral shaft axis was manually defined on a mid-sagittal slice with a line drawn in the center of the femur in a direction parallel to the femoral shaft, and the anterior-posterior (AP_F) axis of the femur was defined by taking the cross product between the ML_F axis and the femoral shaft axis. The superior-inferior (SI_F) axis of the femur was then defined by taking the cross product between the ML_F and AP_F axes, providing a mutually orthogonal set of anatomic axes for the femur.

The segmented femoral bones in the flexed position were rigidly registered to that in the fully extended position by the use of an iterative closest-point shape-matching algorithm, Fig. 5. Thus the femur was held fixed and patellofemoral kinematic parameters and contact area measurements were measured by analyzing the motion of the patella relative to the femoral coordinate system.

The patellofemoral kinematic parameters and contact area measurements were first calculated in each of the two positions, flexed and extended. Patella and contact area positions were recorded based on the FCS and PCS. The kinematic parameters were determined by determining the difference in positions from extended to flexed position.

The patellofemoral kinematic parameters were: (i) Patellar Flexion (rotation of the patella about the ML_F axis,), (ii) Patellar Tilt (rotation of the patella about its long axis, and positive patellar tilt followed the direction of external femoral rotation), (iii) Patellar Rotation (rotation of the patella about the AP_P axis, and positive rotation followed the valgus rotation of femur), Fig. 5. Patellar Translation was determined as three separate parameters with translation of the center of the patella along the AP_F, ML_F, and SI_F axes). Contact area measurements included centroid translation in the AP, ML, and SI direction. The total patellofemoral contact area in the extended and flexed position was also calculated.

2.3. Kinematic MRI reliability testing

An orthopedic surgery resident (rater 1) who previously trained for a year as a radiology resident, and an undergraduate biology student (rater 2) without prior knowledge of anatomy served as raters. The raters met prior to initiating segmentations to establish a standardized approach to identify and separate bony structures and landmarks to guide decision making process during segmentation. For inter-user reliability, all knees were segmented independently and on separate computer monitors. For intra-rater user reliability, rater 1 segmented all knees at a second time point between two and four months after the first segmentation.

2.4. Quantitative (T1ρ) MRI acquisition and processing protocol

T1ρ imaging was acquired on previously established protocols which have been demonstrated to be a reliable method to evaluate cartilage health with excellent reproducibility [26–28,30]. T1ρ mapping for the quantification of cartilage composition consisted of images obtained using FSE images with repetition time (TR) of 3000 ms, echo time (TE) of 9.1 ms, a 512 × 256 matrix, ETL of 16, 16-cms field of view, and 1.5 mms-thick sections with zero spacing. The receiver bandwidth was 64 kHz, and the acquired spin lock times (TSLs) were 0, 10, 40, and 80 ms. Images were obtained at full extension.

Articular cartilage (based on sagittal images were segmented using a spline-based, semiautomatic technique developed in house on the spoiled gradient recalled acquisition in steady state (SPGR)- based on based T1ρ-weighted image with TSL of 0 ms, thus giving the highest signal-to-noise ratio. The T1ρ map was created on a voxel-by-voxel basis using established fitting routines. The segmented masks were overlaid on the T1ρ maps and mean T1ρ values for the entire patella and trochlea regions were calculated. Higher T1ρ relaxation times represent increased cartilage damage.

2.5. Statistical analysis

A priori power analysis was performed to determine the appropriate sample for the study for inter- and intra-rater reliability. Based on data using similar spline-based semi-automated MRI technique for tibiofemoral kinematics with six healthy volunteers that demonstrated kinematic translation calculations had a reproducibility of 0.98 [14], we expected excellent reproducibility. Power calculations performed in G Power (version 3.1.9.2) with alpha = 0.05, beta = 0.95, revealed that a total sample to 12 subjects (eight PFPS and four controls) would be required to account for any potential difficulty with enrolled 10 PFPS and six controls.

Inter- and intra-user reliability was assessed using a two-way random effects model intraclass correlation coefficients (ICC) for each of the patellofemoral kinematic and contact area positions and parameters and measurements. Single measures reliability coefficients and standard error of measurement (SEM) were determined. SEMs were calculated as the standard deviation multiplied with the square root of 1-ICC.

Student's T tests were performed to make comparisons between patellofemoral and control patients. Spearman's correlation was performed to determine the relationship between patellofemoral kinematics and contact area measurements with T1ρ relaxation times. All statistics were performed in SPSS software version 22 (SPSS Inc, Chicago IL) with $p = 0.05$.

3. Results

Sixteen subjects participated in the study (age: 30.8 years (range 24 to 41), eight females). Ten with PFPS were enrolled with mean age 32.3 years (range 27 to 41), with six females. The control group consisted of three females and three males with a mean age 28.6 years (range 24 to 32). There was no significant difference in age between the two groups ($p = 0.11$).

Patellofemoral kinematics and contact area ICC and SEM are demonstrated in Tables 1 and 2. All intra- and inter-user reliability for patello-femoral kinematics was excellent with ICC ≥ 0.843 with $p < 0.001$, Table 1. Inter- and intra-user reliability for patellafemoral contact area was excellent (ICC ≥ 0.8) for seven of 10 measurements with the remaining at good reliability (ICC ≥ 0.725), Table 2.

The mean values and standard deviations for patellofemoral kinematics and contact area measurements are included in Tables 3 and 4, respectively. Patellar tilt in the flexed state was significantly more lateral in PFPS group (3.7°) compared to the controls (8.2°), $p = 0.002$. The patella tilted more laterally in the PFPS group (−1.4°) compared to controls (4.4°) when moving from the extended to flexed position, $p = 0.006$. The patella translated to a more superior position in relation to the femur in the flexed knee of PFPS patients vs controls, $p = 0.032$. There were no significant differences in contact area measurements between PFPS and control groups.

The mean T1ρ relaxation time for control patients in the patellar and trochlear cartilage was 44.8 ms ± 3.3 and 48.9 ± 4.8, respectively. In PFPS patients the mean T1ρ relaxation times for patellar cartilage was 46.9 ms ± 4.4 and trochlear cartilage was 48.0 ms ± 7.6. There were no significant differences between groups for patellar ($p = 0.65$) and trochlear ($p = 0.44$) cartilage. There were no significant correlations between patellofemoral kinematic parameters and contact area measurements and T1ρ relaxation times, $p > 0.05$.

4. Discussion

The most important finding of this study confirmed our primary hypothesis that a spline-based semi-automated kinematic MRI technique to measure patellofemoral kinematics and

contact area measurements demonstrated an excellent level of inter- and intra-user reliability.

Kinematic MRI may provide advantages in identifying patients with maltracking and altered patellofemoral kinematics because it provides dynamic analysis. The spline-based, semi-automated MR technique for kinematic quantifications has been validated in tibio-femoral knee kinematics [26–28] and differs from previously published MR based patellofemoral quantifications because it provides highly reproducible information on patellofemoral kinematics and contact area; where many techniques provide information on one or the other. Intraclass coefficients seen in total contact area in the flexed and extended positions were lower than other parameters, however remained good with ICC > 0.7. The described technique has excellent reproducibility with contact area centroid translation in the anterior-posterior, medial-lateral, and superior-inferior directions. Moreover, this technique provides positional and contact area parameters in the extended and flexed knee positions, which can be used to evaluate static position at extension and flexion. This technique may also be more reproducible as it was tested on 3 T MR scanners, which have become the standard of care in musculoskeletal imaging, compared to prior studies that utilized 1.5 T or less MR scanners and have not been tested on 3 T MR scanners [9,20,23,30,31].

It is also important to note that the second rater was an undergraduate biology student with limited knowledge of anatomy or MR imaging. Her training consisted of a short discussion and demonstration (30 min) of how to properly segment the patella, femur, femoral condyle, patellar axis, femur axis, and patellofemoral contact areas. The excellent inter-user reliability despite the lack of prior anatomy or clinical training of one of the raters highlights the ability of this technique to be used by those who are not trained radiologist or clinicians.

Additionally, our second hypothesis that PFPS patients would have greater lateral translation from extension to flexion was not confirmed. The current study did find that PFPS patients had greater patellar and greater superior patellar translation from extension to flexion compared to controls, however, the remaining patellofemoral kinematics and contact area measurements between PFPS and healthy controls were not significantly different which corresponds with prior research in patellofemoral pain [17]. MacIntyre et al. selected PFPS patients based on history and physical exam and found no differences in patellar spin (rotation), tilt, and lateral translation between PFPS and healthy controls across knee flexion ranges −4 to 60°, except for more lateral patellar translation at 19° of flexion in the PFPS group [17]. This is in contrast to the study that identified more lateral patellar displacement and patellar tilt in PFPS patients compared to healthy controls that defined patellar maltracking in adolescent patients with known history of patellar dislocation [23]. An explanation for our findings is that patients with PFPS in our study were determined to have maltracking based primarily on patellar tilt on merchant view radiographs and although this is a common method used in clinical practice to determine maltracking, this may not be accurate. As such, the PFPS patients in this study may not represent a group of patients with maltracking. This highlights the difficulty of diagnosing patients with true patellofemoral maltracking. Computerized tomography (CT) scans of the patellofemoral joint at 0°, 15°, 30°, and 45° knee flexion has been found to be sensitive to the evaluation of patellar instability [2,11], however dynamic MR based kinematics may also serve as a non-invasive,

in-vivo method to measure patellofemoral maltracking while simultaneously providing information on cartilage and other possible soft tissue etiologies of knee pain.

The third aim for this study to correlate patellofemoral kinematics and contact area with cartilage degeneration of the lateral facet was not confirmed. This study was unique in that it was the first to evaluate cartilage degeneration with T1ρ relaxation times in the patellar and trochlear cartilage to evaluate for a relationship with MR based patellofemoral kinematics or contact area. The lack of relationship of MR based patellofemoral kinematics and cartilage degeneration in this study may also be a result of our patients not truly representing patients with patellofemoral maltracking. Our findings, however, do correspond with a prior study that demonstrated whole patellar and trochlear cartilage does not correlate with patellar tilt determined by merchant view radiographs [29]. It is important to note, that the prior study did find that greater lateral patella tilt correlated with greater T1ρ relaxation times (greater cartilage degeneration) of the lateral facet of the patella only [29]. Our current T1ρ imaging protocol, however, did not permit the patellar cartilage to be split into medial and lateral facets for analysis.

4.1. Limitations

There are several limitations in our study. The knee was flexed at only 30° or at a point of early contact between the patella and femur, where maximum contact between patella and trochlea occurs at 45° flexion. Thirty degrees was chosen to provide easier use of the loading apparatus within MRI scanner. A higher degree of flexion may increase contact area measurements and also improve reproducibility of total contact area measurements. Moreover, the MRI apparatus did not permit true full weight bearing conditions to provide patient comfort and permit image acquisition but may have limited ability to assess patellofemoral kinematics. In a loaded condition, there may greater forces and contact area between the patella and femur. Additionally, our T1ρ quantification protocol did not allow for segmentation of medial and lateral facets of the patellar cartilage which may have limited our ability to detect differences in PFPS and healthy control groups. A prior study that separated medial and lateral facets identified greater cartilage degeneration in the lateral facet [30]. The current study is also limited in our selection of patients with patellofemoral maltracking with radiographs, which may not have truly differentiated PFPS due to maltracking.

5. Conclusions

We demonstrate that spline-based in-vivo patellofemoral kinematic MRI technique to evaluate patellofemoral joint kinematics and contact area has excellent inter- and intra-user reliability.

6. Future directions

Future research should assess anterior knee pain in a larger patient cohort to determine kinematic and contact area parameters to define patellofemoral maltracking with the described in-vivo spline-based semi-automated MRI technique. Potential future studies may assess patients before and after surgical procedures known to alter patellofemoral kinematic

such as Fulkerson osteotomy, anterior cruciate ligament reconstruction, or knee arthroplasty [6,10,21].

References

[1]. Aderinto J, Cobb AG. Lateral release for patellofemoral arthritis. Arthroscopy. 2002; 18(4):399–403. [PubMed: 11951199]

[2]. Biedert RM, Gruhl C. Axial computed tomography of the patellofemoral joint with and without quadriceps contraction. Arch Orthop Trauma Surg. 1997; 116:77–82. [PubMed: 9006771]

[3]. Borotikar BS, Sheehan FT. In vivo patellofemoral contact mechanics during extension using a novel dynamic MRI-based methodology. Osteoarthritis Cartilage. Dec; 2013 31(12):1886–94. [PubMed: 24012620]

[4]. Buck D, Fulkerson J. Anteromedialization of the tibial tubercle: a 4- to 12-year follow-up. Operative Techniques in Sports Medicine. 2000; (8):131–7.

[5]. Buckwalter JA, Mankin HJ, Grodzinksy AJ. Articular cartilage and osteoarthritis. Instr Course Lect. 2005; 54:465–80. [PubMed: 15952258]

[6]. Culvenor AG, Cook JL, Collins NJ, Crossley KM. Is patellofemoral joint osteoarthritis an under-recognized outcome of anterior cruciate ligament reconstruction? A narrative literature review. Br J Sports Med. Jan; 2013 47(2):66–70. [PubMed: 23038783]

[7]. David-Vaudey E, Ghosh S, Ries M, Majumdar S. T2 relaxation time measurements in osteoarthritis. Magn Reson Imaging. 2004; 22:673–82. PubMed: 15172061. [PubMed: 15172061]

[8]. Duncan R, Hay E, Saklatvala J, et al. Prevalence of radiographic osteoarthritis: it all depends on your point of view. Rheumatology. 2006; 45:757–60. [PubMed: 16418199]

[9]. Freedman BR, Sheehan FT. Predicting three-dimensional patellofemoral kinematics from static imaging-based alignment measures. J Orthop Res. Mar; 2013 31(3):441–7. [PubMed: 23097251]

[10]. Fulkerson JP. Anteromedialization of the tibial tuberosity for patellofemoral malalignment. Clin Orthop Relat Res. 1983; (177):176–81. [PubMed: 6861394]

[11]. Goutallier D, Bernageau J, Lecudonnec B. The measurement of the tibial tuberosity. Patella groove distance technique and results. Rev Chir Orthop Reparatrice Appar Mot. 1978; 64:423–8. French. [PubMed: 152950]

[12]. Hunter DJ, March L, Sambrook PN. The association of cartilage volume with knee pain. Osteoarthritis Cartilage. 2003; 11:725–9. [PubMed: 13129691]

[13]. Kornaat P, Bloem J, Ceulemans R, et al. Osteoarthritis of the knee: association between clinical features and MR imaging findings. Radiology. 2006; 239:811–7. [PubMed: 16714463]

[14]. Lansdown DA, Zaid M, Pedoia V, Subburaj K, Souza R, Benjamin C, et al. Reproducibility measurements of three methods for calculating in vivo MR-based knee kinematics. J Magn Reson Imaging. Aug; 2015 42(2):533–8. [PubMed: 25545617]

[15]. LaBella C. Patellofemoral pain syndrome: evaluation and treatment. Prim Care. 2004; 31(4):977–1003. [PubMed: 15544830]

[16]. Li X, Ma B, Link TM, Castillo DD, Blumenkrantz G, Lozano J, et al. In vivo T1ρ and T2 mapping of articular cartilage in osteoarthritis of the knee using 3 T MRI. Osteoarthritis Cartilage. 2007:789–97. [PubMed: 17307365]

[17]. MacIntyre NJ, Hil NA, Fellows RA, Ellis RE, Wilson DR. Patellofemoral joint kinematics in individuals with and without patellofemoral pain syndrome. J Bone Joint Surg Am. Dec; 2006 88(12):2596–605. [PubMed: 17142409]

[18]. McWalter EJ, O'Kane CM, Fitzpatrick DP, Wilson DR. Validation of an MRI-based method to assess patellofemoral joint contact areas in loaded knee flexion in vivo. J Magn Reson Imaging. Apr; 2014 39(4):978–87. [PubMed: 24006182]

[19]. Natoli RM, Athanasiou KA. Traumatic loading of articular cartilage: mechanical and biological responses and post-injury treatment. Biorheology. 2009; 46:451–85. [PubMed: 20164631]

[20]. Pal S, Besier TF, Beaupre GS, Fredericson M, Delp SL, Gold GE. Patellar maltracking is prevalent among patellofemoral pain subjects with patella alta: an upright, weightbearing MRI study. J Orthop Res. Mar; 2013 31(3):448–57. [PubMed: 23165335]

[21]. Petersen W, Rembitzki IV, Bruggemann GP, Ellermann A, Best R, Koppenburg AG, et al. Anterior knee pain after total knee arthroplasty: a narrative review. Int Orthod. Feb; 2014 38(2): 319–28.

[22]. Powers CM, Bolgla LA, Callaghan MJ, Collins N, Sheehan FT. Patellofemoral pain: proximal, distal, and local factors, 2nd International Research Retreat. J Orthop Sports Phys Ther. 2012; 42:A1–A54. [PubMed: 22660660]

[23]. Regalado G, Lintula H, Eskelinen M, Kokki H, Kroger H, Svedstrom E. Dynamic KINE-MRI in patellofemoral instability in adolescents. Knee Surg Sports Traumatol Arthrosc. 2014; 22(11): 2795–802. [PubMed: 24045916]

[24]. Regatte RR, Akella SVS, Wheaton AJ, Lech G, Borthakur A, Kneeland JB, et al. 3D-T1ρ-relaxation mapping of articular cartilage: in vivo assessment of early degenerative changes in symptomatic osteoarthritic subjects. Acad Radiol. 2004; 11:741–9. PubMed: 15217591. [PubMed: 15217591]

[25]. Shea KP, Fulkerson JP. Preoperative computed tomography scanning and arthroscopy in predicting outcome after lateral retinacular release. Arthroscopy. 1992; 8(3):327–34. 26:289–96. [PubMed: 1418204]

[26]. Souza RB, Baum T, Wu S, Feeley BT, Kadel N, Li X, et al. Effects of unloading on knee articular cartilage T1rho and T2 magnetic resonance imaging relaxation times: a case series. J Orthop Sports Phys Ther. 2012; 42:511–20. [PubMed: 22402583]

[27]. Souza RB, Fang C, Luke A, Wu S, Li X, Majumdar S. Relationship between knee kinetics during jumping tasks and knee articular cartilage MRI T1rho and T2 relaxation times. Clin Biomech (Bristol, Avon). 2012; 27:403–8.

[28]. Souza RB, Wu SJ, Lee JM, Subburaj K, Allen CR, Feeley BT. Cartilage MRI relaxation times after arthroscopic partial medial meniscectomy reveal localized degeneration. Knee Surg Sports Traumatol Arthrosc. 2015; 23(1):188–97. [PubMed: 24792070]

[29]. Szebenyi B, Hollander A, Dieppe P, et al. Associations between pain, function, and radiographic features in osteoarthritis of the knee. Arthritis Rheum. 2006; 54:230–5. [PubMed: 16385522]

[30]. Thuillier DU, Souza RB, Wu S, Luke A, Li X, Feeley BT. T1ρ imaging demonstrates early changes in the lateral patella in patients with patellofemoral pain and maltracking. Am J Sports Med. 2013:1813–1818. [PubMed: 23845401]

[31]. von Eisenhart-Rothe R, Lenze U, Hinterwimmer S, Pohlig F, Graichen H, Stein T, et al. Tibiofemoral and patellofemoral joint 3D kinematics in patients with posterior cruciate ligament deficiency compared to healthy volunteers. BMC Musculoskelet Disord. Nov 26.2012 13:231. [PubMed: 23181354]

[32]. Westhpal CJ, Schmitz A, Reeder SB, Thelen DG. Load-dependent variations in knee kinematics measured with dynamic MRI. J Biomech. Aug 9; 2013 46(12):2045–52. [PubMed: 23806309]

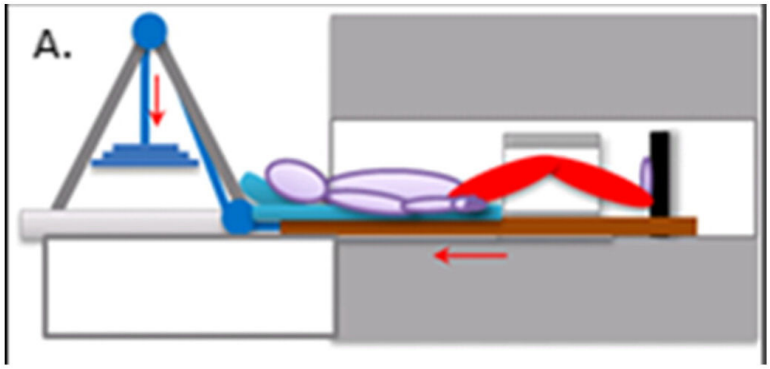

Fig. 1.

Kinematic loading apparatus. Schematic demonstrating in-house built loading apparatus mounted on a scanner with 25% of subject weight load applied. Figure demonstrates patient's knee in flexed position only, but the apparatus is used similarly in full extended position.

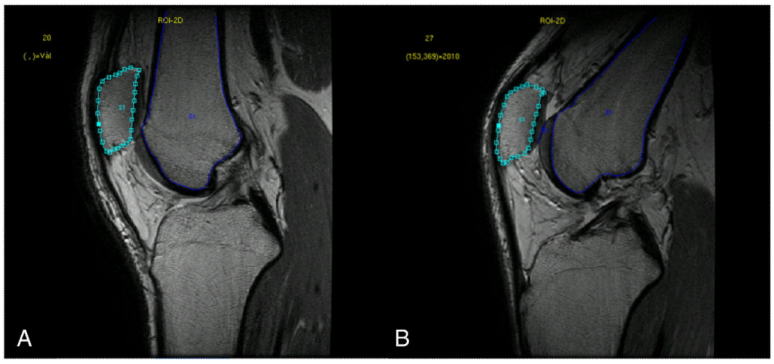

Fig. 2.

Fast spin echo fat-saturated MR image segmentation of patella and femur with spline based segmentation of regions of interest using in-house built MATLAB based program. (A) Extended state and (B) flexed state.

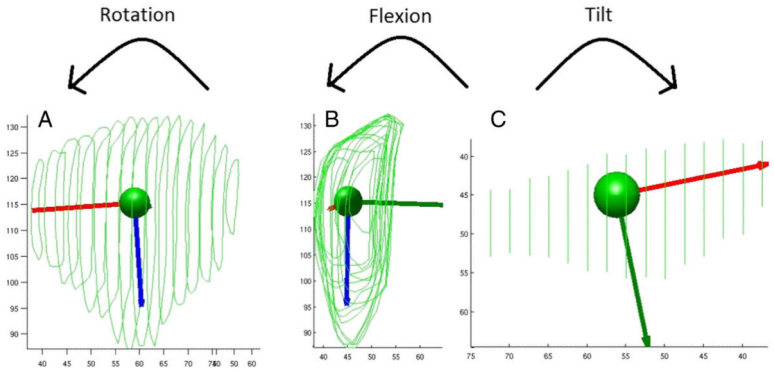

Fig. 3.

Patellar coordinate system and kinematics parameters. Patellar coordinate system and kinematics parameters (A) frontal view, (B) sagittal view, and (C) transverse view. Lines represent anterior-posterior, medial-lateral, and superior-inferior axes of rotation. Arrows signify direction of positive (medial rotation, inferior flexion, and medial tilt.

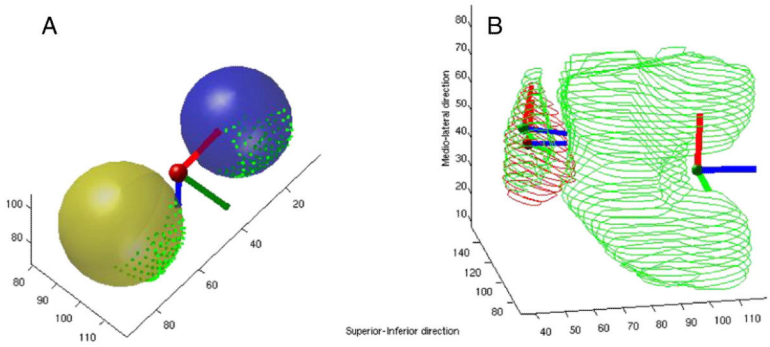

Fig. 4.

Femoral coordinate system. Femoral coordinate system is based on spheres of medial and lateral femoral condyles. (A) Shows schematic of coordinate system centered in spheres of femoral condyles. (B) Shows schematic with femoral coordinate system in place of anatomic femur.

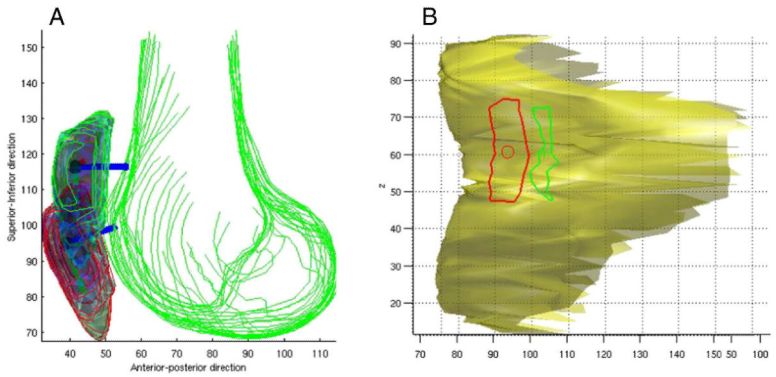

Fig. 5.

Kinematic and contact area registration. (A) Schematic demonstrating rigid registration of femurs in flexed and extended states, allowing for calculation of patellar position in each state and patellar motion between flexed and extended states. (B) Schematic showing contact patellofemoral contact area with femur rigidly registered.

Table 1

Patellar Kinematics Intra-user was performed 2–3 months apart by a single user and inter-user was performed by two separate individuals over the same time span.

	Intra-user	SEM (intra)	Inter-user	SEM (inter)
Patella flexion [deg] (extended to flexed position)	0.98*	1.56	0.99*	0.85
Patella flexion [deg] (extended position)	0.93*	1.68	0.87*	2.48
Patella flexion [deg] (flexed position)	0.91*	2.40	0.87*	2.57
Patella tilt [deg] (extended to flexed position)	0.97*	0.81	0.94*	1.21
Patella tilt [deg] (extended position)	0.85*	1.23	0.90*	1.12
Patella tilt [deg] (flexed position)	0.93*	0.98	0.90*	1.26
Patella rotation [deg] (extended to flexed position)	0.84*	1.34	0.87*	1.25
Patella rotation [deg] (extended position)	0.85*	1.71	0.98*	0.55
Patella rotation [deg] (flexed position)	0.92*	0.94	0.87*	1.16
Patella translation (AP) [mm] (extended to flexed position)	0.87*	1.50	0.96*	0.73
Patella translation (AP) [mm] (extended position)	0.95*	2.40	0.97*	1.87
Patella translation (AP) [mm] (flexed position)	0.98*	1.67	0.99*	1.30
Patella translation (ML) [mm] (extended to flexed position)	0.91*	1.25	0.96*	0.90
Patella translation (ML) [mm] (extended position)	0.99*	0.60	0.99*	0.70
Patella translation (ML) [mm] (flexed position)	0.99*	1.10	0.99*	0.65
Patella translation (SI) [mm] (extended to flexed position)	0.94*	1.60	0.97*	1.15
Patella translation (SI) [mm] (extended position)	0.99*	1.45	0.99*	1.28
Patella translation (SI) [mm] (flexed position)	−0.99*	1.43	0.99*	0.95

SEM = Standard Error of Measurement.

* $p \leq 0.0001$.

Table 2

Patellofemoral contact area intraclass correlation coefficients.

	Intra-user	SEM (intra)	Inter-user	SEM (inter)
Contact area extended (mm^2)	0.79*	34.91	0.78*	36.33
Contact area flexed (mm^2)	0.74*	41.89	0.73*	40.95
Centroid translation (AP) [mm] (extended to flexed position)	0.96*	0.44	0.93*	0.59
Centroid translation (AP) [mm] (extended position)	0.96*	0.60	0.90*	0.99
Centroid translation (AP) [mm] (flexed position)	0.95*	0.76	0.97*	0.62
Centroid translation (ML) [mm] (extended to flexed position)	0.75*	2.24	0.94*	1.21
Centroid translation (ML) [mm] (extended position)	0.92*	2.38	0.96*	1.74
Centroid translation (ML) [mm] (flexed position)	0.97*	1.28	0.98*	0.90
Centroid translation (SI) [mm] (extended to flexed position)	0.81*	1.62	0.77*	1.95
Centroid translation (SI) [mm] (extended position)	0.92*	1.27	0.82*	1.88
Centroid translation (SI) [mm] (flexed position)	0.95	0.76	0.97*	0.62

Patellofemoral contact area kinematics intra-user was performed two to three months apart by a single user and inter-user was performed by two separate individuals over the same time span.

SEM = standard error of measurement.

* $p \leq 0.0001$.

Table 3

Patellofemoral kinematics patellofemoral pain vs healthy control.

	Mean PFPS (SD)	Mean control (SD)	T-test
Patellar flexion [deg] (extended to flexed position)	13.8	19.7	0.14
Patellar flexion [deg] (extended position)	6.7	6.9	0.95
Patellar flexion [deg] (flexed position)	20.5	26.6	0.13
Patellar tilt [deg] (extended to flexed position)	−1.4	4.4	0.006
Patellar tilt [deg] (extended position)	5.1	3.9	0.48
Patellar tilt [deg] (flexed position)	3.7	8.2	0.002
Patellar rotation [deg] (extended to flexed position)	−3.0	−3.8	0.72
Patellar rotation [deg] (extended position)	6.3	9.6	0.16
Patellar rotation [deg] (flexed position)	3.3	5.8	0.15
Patellar translation (AP) [mm] (Extended to flexed position)	1.6	2.9	0.54
Patellar translation (AP) [mm] (extended position)	34.0	36.9	0.58
Patellar translation (AP) [mm] (flexed position)	35.6	39.8	0.43
Patellar translation (ML) [mm] (extended to flexed position)	−0.05	−0.4	0.90
Patellar translation (ML) [mm] (extended position)	47.2	43.2	0.43
Patellar translation (ML) [mm] (flexed position)	47.1	42.8	0.38
Patellar translation (SI) [mm] (extended to flexed position)	17.2	22.0	0.15
Patellar translation (SI) [mm] (extended position)	−108.3	−99.3	0.20
Patellar translation (SI) [mm] (flexed position)	−91.1	−77.3	0.03

Table 4

Patello-femoral contact area PFPS vs control.

	Mean PFPS (SD)	Mean control (SD)	T-test
Contact area extended (mm^2)	186.5	123.3	0.18
Contact area flexed (mm^2)	317.3	237.6	0.09
Centroid translation (AP) [mm] (extended to flexed position)	1.4	2.4	0.42
Centroid translation (AP) [mm] (extended position)	−43.0	−43.4	0.79
Centroid translation (AP) [mm] (flexed position)	−41.6	−41.1	0.76
Centroid translation (ML) [mm] (extended to flexed position)	−0.9	−1.1	0.94
Centroid translation (ML) [mm] (extended position)	7.7	5.5	0.70
Centroid translation (ML) [mm] (flexed position)	4.7	6.6	0.64
Centroid translation (SI) [mm] (extended to flexed position)	−10.3	−11.3	0.63
Centroid translation (SI) [mm] (extended position)	9.1	8.4	0.79
Centroid translation (SI) [mm] (flexed position)	−41.6	−41.1	0.76

Patello-femoral pain patients vs healthy controls.

PFPS = Patellofemoral pain syndrome.

Positive numbers (+) refer to posterior, medial, or inferior motion.

Negative numbers (−) refer to anterior, lateral, or superior motion.